

may explain why it has not been possible to purify an intact, active CSC. Although S-acylation is known to affect partitioning of proteins into membrane microdomains, it has also been suggested that the crowding of S-acyl groups within a membrane may actually facilitate the formation of lipid microdomains (19). The high level of S-acylation found in the CSC would make it a very good candidate for a protein complex capable of generating lipid microdomains that may facilitate the colocalization of proteins with similar properties. We note that a recent proteomic study of S-acylated proteins also identified the endoglucanase KORRIGAN, a known CESA-binding protein (5).

REFERENCES AND NOTES

1. A. N. Fernandes et al., *Proc. Natl. Acad. Sci. U.S.A.* **108**, E1195–E1203 (2011).
2. A. R. Paredes, C. R. Somerville, D. W. Ehrhardt, *Science* **312**, 1491–1495 (2006).
3. F. Diotallevi, B. Mulder, *Biophys. J.* **92**, 2666–2673 (2007).
4. P. A. Hemsley, *New Phytol.* **205**, 476–489 (2015).
5. P. A. Hemsley, T. Weimar, K. S. Lilley, P. Dupree, C. S. Grierson, *New Phytol.* **197**, 805–814 (2013).
6. M. Kumar, S. Turner, *Phytochemistry* **112**, 91–99 (2015).
7. M. T. Forrester et al., *J. Lipid Res.* **52**, 393–398 (2011).
8. C. E. Vergara, N. C. Carpita, *Plant Mol. Biol.* **47**, 145–160 (2001).
9. R. Wightman, S. R. Turner, *Plant J.* **54**, 794–805 (2008).
10. Y. Watanabe et al., *Science* **350**, 198–203 (2015).
11. E. F. Crowell et al., *Plant Cell* **21**, 1141–1154 (2009).
12. R. Gutierrez, J. J. Lindeboom, A. R. Paredes, A. M. C. Emons, D. W. Ehrhardt, *Nat. Cell Biol.* **11**, 797–806 (2009).
13. N. G. Taylor, R. M. Howells, A. K. Huttly, K. Vickers, S. R. Turner, *Proc. Natl. Acad. Sci. U.S.A.* **100**, 1450–1455 (2003).
14. L. Sethaphong et al., *Proc. Natl. Acad. Sci. U.S.A.* **110**, 7512–7517 (2013).
15. J. L. W. Morgan, J. Strumillo, J. Zimmer, *Nature* **493**, 181–186 (2013).
16. S. Monier, D. J. Dietzen, W. R. Hastings, D. M. Lublin, T. V. Kurzchalia, *FEBS Lett.* **388**, 143–149 (1996).
17. O. Batistic, N. Sorek, S. Schultke, S. Yalovsky, J. Kudla, *Plant Cell* **20**, 1346–1362 (2008).
18. I. I. Atanassov II, J. K. Pittman, S. R. Turner, *J. Biol. Chem.* **284**, 3833–3841 (2009).
19. S. S. A. Konrad, T. Ott, *Trends Plant Sci.* **20**, 351–361 (2015).

ACKNOWLEDGMENTS

We thank J. Ogas for a critical reading of the manuscript. H. Höfte kindly provided antibodies against CESA1 and CESA6. The work was funded by Biotechnology and Biological Sciences Research Council grants BB/H012923/1 and BB/M004031/1 to S.T. and BB/M024911/1 to P.A.H. The Microscopy Facility at the Sainsbury Laboratory is supported by the Gatsby Charitable Foundation. The authors declare no conflict of interest. M.K., R.W., I.A., A.G., C.H.H., and P.A.H. carried out the experimental work. M.K., P.A.H., and S.T. wrote the manuscript and conceived the experiments. Supplementary materials contain additional data. S.T. would like to dedicate this manuscript to physicist Roy Turner (1931–2016) for his support, encouragement, and help with advanced mathematics.

SUPPLEMENTARY MATERIALS

www.sciencemag.org/content/353/6295/166/suppl/DC1
Materials and Methods
Figs. S1 to S8
Tables S1 and S2
Movies S1 to S3
References (20–25)

5 February 2016; accepted 6 June 2016
10.1126/science.aaf4009

CLIMATE CHANGE

Climate-driven regime shift of a temperate marine ecosystem

Thomas Wernberg,^{1,*†} Scott Bennett,^{1,2,3,†} Russell C. Babcock,^{1,4} Thibaut de Bettignies,^{1,5} Katherine Cure,^{1,6} Martial Depeczynski,⁶ Francois Dufois,⁷ Jane Fromont,⁸ Christopher J. Fulton,⁹ Renae K. Hovey,¹ Euan S. Harvey,² Thomas H. Holmes,^{1,10} Gary A. Kendrick,¹ Ben Radford,^{6,11} Julia Santana-Garcon,^{1,2,3} Benjamin J. Saunders,² Dan A. Smale,^{1,12} Mads S. Thomsen,^{1,13} Chenae A. Tuckett,¹ Fernando Tuya,^{1,4} Mathew A. Vanderklift,⁷ Shaun Wilson^{1,10}

Ecosystem reconfigurations arising from climate-driven changes in species distributions are expected to have profound ecological, social, and economic implications. Here we reveal a rapid climate-driven regime shift of Australian temperate reef communities, which lost their defining kelp forests and became dominated by persistent seaweed turfs. After decades of ocean warming, extreme marine heat waves forced a 100-kilometer range contraction of extensive kelp forests and saw temperate species replaced by seaweeds, invertebrates, corals, and fishes characteristic of subtropical and tropical waters. This community-wide tropicalization fundamentally altered key ecological processes, suppressing the recovery of kelp forests.

Broad-scale losses of species that provide the foundations for habitats cause dramatic shifts in ecosystem structure, because they support core ecological processes (1–3). Such habitat loss can lead to a regime shift, in which reinforcing feedback mechanisms intensify to provide resilience to an alternate community configuration, often with profound ecological, social, and economic consequences (4–6). Benthic marine regime shifts have been associated with the erosion of ecological resilience through overfishing or eutrophication, altering the balance between consumers and resources, rendering ecosystems vulnerable to major disturbances (1, 2, 6, 7).

¹School of Plant Biology and Oceans Institute, The University of Western Australia, 39 Fairway, Crawley, Western Australia 6009, Australia. ²Department of Environment and Agriculture, School of Science, Curtin University, Bentley, Western Australia 6102, Australia. ³Department of Global Change Research, Institut Mediterrani d'Estudis Avançats (Universitat de les Illes Balears–Consejo Superior de Investigaciones Científicas), Esporles, Spain. ⁴Commonwealth Scientific and Industrial Research Organisation (CSIRO) Oceans and Atmosphere, General Post Office Box 2583, Brisbane, Queensland 4001, Australia. ⁵Service du Patrimoine Naturel, Muséum National d'Histoire Naturelle, 36 Rue Geoffroy Saint-Hilaire CP41, Paris 75005, France. ⁶Australian Institute of Marine Science, 39 Fairway, Crawley, Western Australia 6009, Australia. ⁷CSIRO Oceans and Atmosphere Flagship, Private Bag 5, Wembley, Western Australia 6913, Australia. ⁸Western Australian Museum, Locked Bag 49, Welshpool DC, Western Australia 6986, Australia. ⁹Research School of Biology, The Australian National University, Canberra, Australian Capital Territory 2601, Australia. ¹⁰Marine Science Program, Science Division, Department of Parks and Wildlife, Kensington, Western Australia 6151, Australia. ¹¹School of Geography and Environmental Science, The University of Western Australia, 39 Fairway, Crawley, Western Australia 6009, Australia. ¹²Marine Biological Association of the United Kingdom, The Laboratory, Citadel Hill, Plymouth PL1 2PB, UK. ¹³Marine Ecology Group, School of Biological Sciences, The University of Canterbury, Private Bag 4800, Christchurch, New Zealand. ¹⁴Instituto Universitario Ecoaquia, Universidad de Las Palmas de Gran Canaria, 35017 Canary Islands, Spain.

*Corresponding author. Email: thomas.wernberg@uwa.edu.au

†These authors contributed equally to this work. The other authors are arranged alphabetically.

Now, climate change is also contributing to the erosion of resilience (8, 9), because increasing temperatures are modifying key physiological, demographic, and community-scale processes (8, 10), driving species redistribution at a global scale and rapidly breaking down long-standing biogeographic boundaries (11, 12). These processes culminate in novel ecosystems where tropical and temperate species interact, with unknown implications (13). Here we document how a marine heat wave caused the loss of kelp forests across ~2300 km² of Australia's Great Southern Reef, forcing a regime shift to seaweed turfs. We describe a rapid 100-km range contraction of kelp forests and a community-wide shift toward warm-water species, with ecological processes suppressing kelp forest recovery.

To document ecosystem changes, we surveyed kelp forests, seaweeds, fish, mobile invertebrates, and corals at 65 reefs across a ~2000-km tropical-to-temperate transition zone in western Australia (14). Surveys were conducted between 2001 and 2015, covering the years before and after an extreme marine heat wave affected the region.

The Indian Ocean adjacent to western Australia is a “hot spot” where the rate of ocean warming is in the top 10% globally (15), and isotherms are shifting poleward at a rate of 20 to 50 km per decade (16). Until recently, kelp forests were dominant along >800 km of the west coast (8), covering 2266 km² of rocky reefs between 0 and 30 m depth south of 27.7°S (Fig. 1). Kelp forests along the mid-west section of this coast (27.7° to 30.3°S) have experienced steadily increasing ocean temperatures since the 1970s, recently punctuated by three of the warmest summers in the past 215 years (Fig. 2) (17, 18, 19). In December 2010, immediately before an extreme marine heat wave, kelp forests covered over ~70% of shallow rocky reefs in the midwest (Fig. 2 and fig. S1), with no differences in kelp cover or biomass among reefs along the west coast (Fig. 1 and figs. S1 and S2) (8). During this time, seaweed and fish communities in the

midwest were similar to those of the temperate southwest (~500 km farther south) and clearly distinct from those of tropical reefs in the (~500 km farther north) (Fig. 3, A and B, and fig. S3) (17).

By early 2013, only 2 years later, our extensive surveys found a 43% (963 km²) loss of kelp forests on the west coast (Fig. 1). Previously dense kelp forests north of 29°S had disappeared (Fig. 2 and fig. S1) or been severely reduced (>90% loss, Fig. 1), representing a ~100-km range contraction and functional extinction from 370 km² of reef (a reduction in abundance severe enough to delete ecological function). Instead, we found a dramatic increase in the cover of turf-forming seaweeds (Fig. 2) and a community-wide shift from species characteristic of temperate waters to species and functional groups characteristic of subtropical and tropical waters [Figs. 3 and 4 and fig. S3, mean square contingency coefficient ($\phi_{2,52}$) = -0.70, $P < 0.001$]. Compared to the composition of the heavily affected midwest reef communities in Kalbarri before the 2011 marine heat wave, differences in community structure (Bray-Curtis dissimilarity) from reefs in Perth in the temperate southwest increased by 91 and 28% for seaweeds and fishes, respectively, whereas differences from Ningaloo Reef in the tropical northwest decreased by 32 and 16%, respectively. This broad-scale community-wide reef transformation reflected consistent decreases in the abundance of taxa characteristic of temperate reefs, coinciding with increases in the abundance of species characteristic of subtropical and tropical reefs, for both seaweeds (Fig. 3C and table S2, $\phi_{2,20}$ = -0.81, $P < 0.001$) and fishes (Fig. 3D and table S3, $\phi_{2,20}$ = -0.64, $P = 0.008$). Similar changes were seen for sessile and mobile invertebrates in the southern part of the midwest region, where small hermatypic coral colonies increased almost sixfold in abundance and doubled in species richness (Fig. 4 and table S5), while the abundances of sea urchins and gastropods also increased and decreased in accordance with their thermal affinities (Fig. 4 and tables S4 and S5, $\phi_{2,12}$ = -0.68, $P < 0.045$).

Even though the acute climate stressor has abated (Fig. 2 and fig. S1), as of late 2015, almost 5 years after the heat wave, we have observed no signs of kelp forest recovery on the heavily affected reefs north of 29°S. Instead, concurrent with an 80% reduction in standing seaweed biomass (fig. S2), we have recorded subtropical and tropical fish feeding rates on canopy seaweeds that are three times higher than on comparable coral reef systems. Similarly, we have found a 400% increase in the biomass of scraping and grazing fishes, a functional group characteristic of coral reefs, which now display grazing rates on seaweed turfs that are comparable to those observed on healthy coral reefs worldwide (table S6) (10). High herbivore pressure now suppresses the recovery of kelp forests by cropping turfs and kelp recruits (10).

We deduce that extreme temperatures beginning in 2011 exceeded a physiological tipping point for kelp forests north of 29°S, and now reinforcing feedback mechanisms have become established that support a new kelp-free state. Similar ecosystem changes have not been observed in the south-

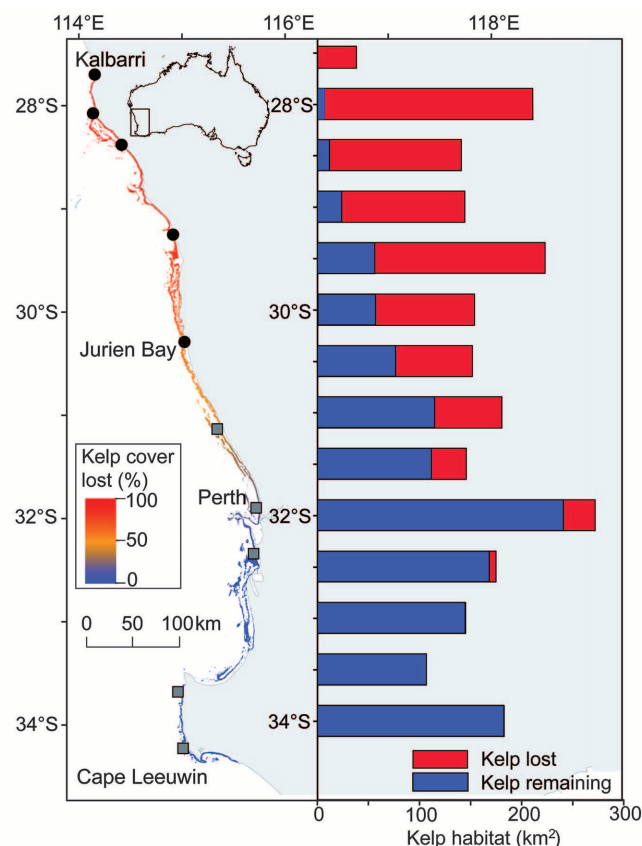


Fig. 1. Extent of kelp forests in western Australia before and after the 2011 marine heat wave. (Left) The extent of kelp forests from 0 to 30 m depth before 2011 is shown (map), with a color scale indicating the proportion lost by 2013. (Right) The area of kelp forests before 2011 in 0.5° bins (bars).

Before 2011, kelp forests covered 2266 km² along the >800 km of coastline. However, by 2013, 43% of these kelp forests had disappeared (red bars). On the left side of the map, gray squares (southwest region) and black circles (midwest region) mark locations where reefs were surveyed by scuba divers to establish proportional kelp loss (table S1).

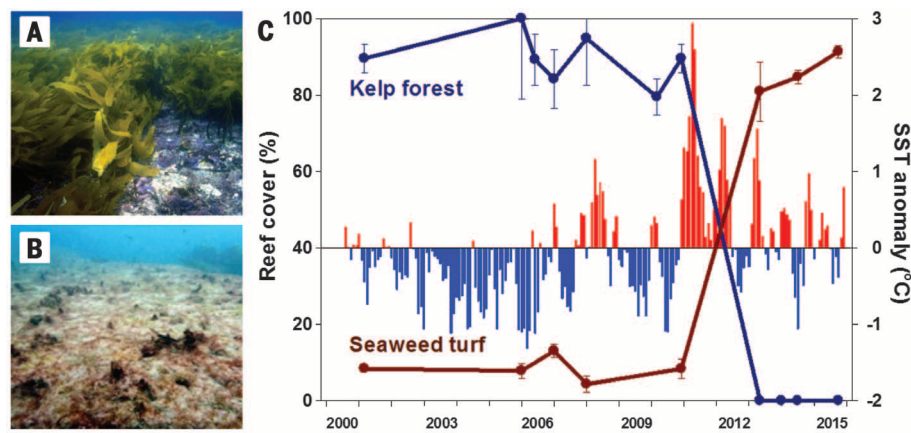


Fig. 2. Regime shift from kelp forests to seaweed turfs after the 2011 marine heat wave. Kelp forests were dense in Kalbarri until 2011 (A), when they disappeared from ~100 km of coastline (Fig. 1) and were replaced by seaweed turfs (B). (C) The habitat transition (lines) coincided with exceptionally warm summers in 2011, 2012, and 2013 (red bars), punctuating gradually increasing mean ocean temperatures over the past decades (17). Shown are mean (\pm SE, $n = 3$ reefs) kelp forest cover (dark blue circles and line) and seaweed turf cover (dark red circles and line), chronologically aligned with monthly sea surface temperature (SST) anomalies (blue and red bars) relative to monthly climatological means for 1981–2015 (table S1).

west, where heat wave temperatures remained within the thermal tolerance of kelps (17), and the greater distance to tropical bioregions limited the incursion of tropical species. Threshold temperatures for kelp forests appear close to 2.5°C above long-term summer maximum temperatures, consistent with other seaweeds in the region (20). However, the partial loss of kelp forests on reefs

between 29° and 32°S suggests that there is variation in threshold temperatures within and between kelp populations.

The consistent responses of both cool- and warm-water species clearly illustrate the important role of temperature. However, the transition in community structure and subsequent persistence of the new regime would have been augmented

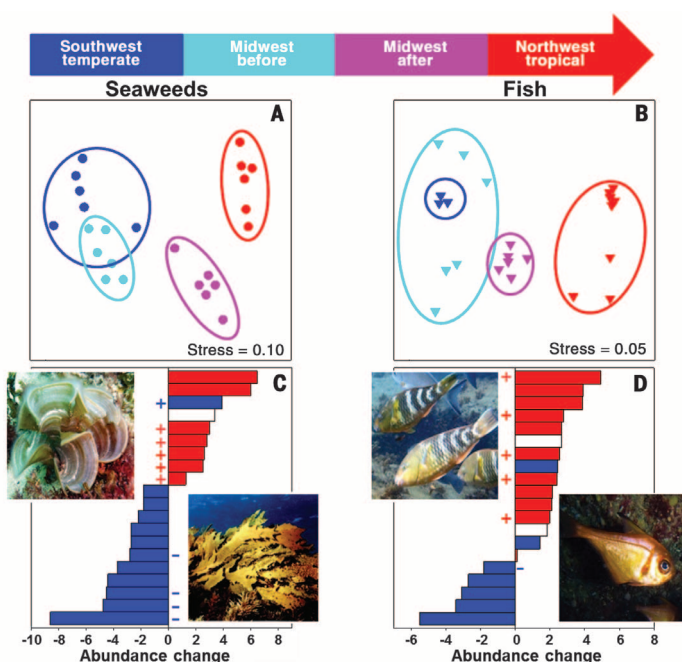


Fig. 3. Changes in seaweed and fish communities on affected reefs after the 2011 marine heat wave. Ordinations (nonmetric multidimensional scaling) of seaweed (A) and fish (B) communities show how community structure on reefs north of 29°S shifted from a close resemblance to temperate reefs farther south to a greater resemblance to tropical reefs to the north. Dark blue = Perth (2005–2007), light blue = Kalbarri before (2005–2007), pink = Kalbarri after (2013–2015), red = Ningaloo Reef (2010) (table S1). Each symbol represents an individual reef. Ordinations are based on Bray-Curtis dissimilarities calculated from $\ln(x + 1)$ -transformed data. (C and D) Change in $\ln(x + 1)$ -transformed abundance of seaweeds [(C) grams of fresh weight per 1.5 m²] and fish [(D) individuals per 2500 m²] in Kalbarri (2005–2007 versus 2013–2015) clearly show the decline in cool-water species (blue bars) and concurrent increase in warm-water species (red bars), with several species not previously recorded (+) or now absent from the samples (–). Each bar represents an average across six reefs for an individual species. White bars indicate taxa with ambiguous distributions. Species are listed in tables S2 and S3.

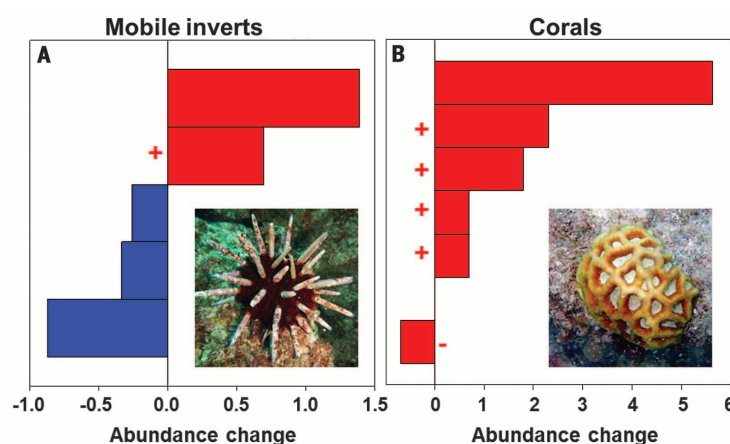


Fig. 4. Changes in benthic invertebrate abundances in the midwest after the 2011 marine heat wave. (A and B) Change in $\ln(x + 1)$ -transformed abundance of common mobile invertebrates (inverts) [(A) individuals per 30 m²] and small (<6 cm) hermatypic corals [(B) colonies per 1000 m²]. Colors and symbols are as in Fig. 3. Each bar represents an average across 6 and 23 reefs for an individual species of mobile invertebrates and corals, respectively. Mobile invertebrates were counted in Jurien Bay (2005, 2011 versus 2013 and 2014), and corals were counted between Cervantes and Dongara (30.6° to 29.3°S) (2005–2006 versus 2013) (table S1). Species are listed in tables S4 and S5.

by the low and high availability of temperate and tropical propagules and immigrants, respectively, as well as changes in competitive interactions after the loss of kelp canopies (27). The oceanography of the region is dominated by the poleward-flowing Leeuwin Current, which delivers warm nutrient-poor water and tropical species into the temperate region, while limiting the supply of propagules, including kelp zoospores from higher-latitude kelp forests (22, 23). Indeed, healthy coral reefs already occur at the Houtman-Abrolhos Islands, 60 km offshore from Kalbarri, directly in the path of the Leeuwin Current. Until now, however, cooler coastal waters have enabled kelp forests to dominate nearshore reefs.

The Leeuwin Current is strongly influenced by the El Niño–Southern Oscillation (24). The strength of the Leeuwin Current and the flow of warm tropical water down the west coast of Australia increase during the La Niña phase of this cycle. These La Niña conditions drive warming anomalies such as the 2011 marine heat wave (24) and are predicted to double in frequency and intensity in the near future (25). Moreover, the southeast Indian Ocean has gradually warmed by at least 0.65°C over the past five decades and will continue to warm until the end of the century and beyond (19). Kelp forest recovery from disturbances can be slow in the nutrient-poor west coast waters, even in the cool southwest (8, 26), providing time for populations of herbivorous fish to become established and seaweed turfs to proliferate. Consequently, the probability of prolonged cool conditions that could reset community structure and ecological processes to facilitate the recovery of kelp forests is becoming increasingly unlikely, while the risk of more heat waves that will exacerbate and expand the new tropicalized ecosystem state is increasing (25).

Short-term climate variability has previously precipitated large-scale destruction of kelp forests (27, 28), which have mostly recovered as environmental conditions returned to normal. The future of kelp forest communities in western Australia is, however, grim. Warming, more frequent heat waves, and the intrusion of tropical species into temperate habitats are unequivocal (13, 19, 25). The current velocity of ocean warming is pushing kelp forests toward the southern edge of the Australian continent (29), where they are at risk of rapid local extinction over thousands of kilometers, due to the east-west orientation of the continent's poleward coastline and west-to-east flow of surface currents (12). This would devastate lucrative fishing and tourism industries worth more than \$10 billion (Australian) per year (30) and have catastrophic consequences for the thousands of endemic species (30) supported by the kelp forests of Australia's Great Southern Reef.

REFERENCES AND NOTES

1. T. P. Hughes, *Science* **265**, 1547–1551 (1994).
2. R. S. Steneck *et al.*, *Environ. Conserv.* **29**, 436–459 (2002).
3. M. S. Thomsen *et al.*, *Integr. Comp. Biol.* **50**, 158–175 (2010).
4. M. Scheffer, S. Carpenter, J. A. Foley, C. Folke, B. Walker, *Nature* **413**, 591–596 (2001).
5. N. A. J. Graham *et al.*, *Front. Ecol. Environ.* **11**, 541–548 (2013).
6. R. S. Steneck, A. Leland, D. C. McNaught, J. Vavrinc, *Bull. Mar. Sci.* **89**, 31–55 (2013).

7. S. D. Ling, C. R. Johnson, S. D. Frusher, K. R. Ridgway, *Proc. Natl. Acad. Sci. U.S.A.* **106**, 22341–22345 (2009).
8. T. Wernberg et al., *Ecol. Lett.* **13**, 685–694 (2010).
9. N. A. J. Graham, S. Jennings, M. A. MacNeil, D. Mouillot, S. K. Wilson, *Nature* **518**, 94–97 (2015).
10. S. Bennett, T. Wernberg, E. S. Harvey, J. Santana-Garcon, B. J. Saunders, *Ecol. Lett.* **18**, 714–723 (2015).
11. E. S. Poloczanska et al., *Nat. Clim. Change* **3**, 919–925 (2013).
12. T. Wernberg et al., *Curr. Biol.* **21**, 1828–1832 (2011).
13. A. Vergés et al., *Proc. Biol. Sci.* **281**, 20140846 (2014).
14. Materials and methods are available as supplementary materials on Science Online.
15. A. Hobday, G. Pecl, *Rev. Fish Biol. Fish.* **24**, 415–425 (2014).
16. M. T. Burrows et al., *Science* **334**, 652–655 (2011).
17. T. Wernberg et al., *Nat. Clim. Change* **3**, 78–82 (2013).
18. J. Zinke et al., *Nat. Commun.* **5**, 3607 (2014).
19. J. Lough, A. Sen Gupta, A. J. Hobday, in *Report Card of Marine Climate Change for Australia: Detailed Scientific Assessment*, E. S. Poloczanska, A. J. Hobday, A. J. Richardson, Eds. (Hobart, Tasmania, 2012); www.oceanclimatechange.org.au.
20. S. Bennett, T. Wernberg, B. Arackal Joy, T. de Bettignies, A. H. Campbell, *Nat. Commun.* **6**, 10280 (2015).
21. D. P. Thomson, R. C. Babcock, M. A. Vanderklift, G. Symonds, J. R. Gunson, *Estuar. Coast. Shelf Sci.* **96**, 105–113 (2012).
22. M. Feng, D. Slawinski, L. E. Beckley, J. K. Keesing, *Mar. Freshw. Res.* **61**, 1259–1267 (2010).
23. M. A. Coleman et al., *J. Ecol.* **99**, 1026–1032 (2011).
24. M. Feng, M. J. McPhaden, S.-P. Xie, J. Hafner, *Scientific Reports* **3**, 1277 (2013).
25. W. Cai et al., *Nat. Clim. Change* **5**, 132–137 (2015).
26. B. D. Toohy, G. A. Kendrick, E. S. Harvey, *Oikos* **116**, 1618–1630 (2007).
27. P. K. Dayton, M. J. Tegner, *Science* **224**, 283–285 (1984).
28. E. A. Martinez, L. Cardenas, R. Pinto, *J. Phycol.* **39**, 504–508 (2003).
29. M. T. Burrows et al., *Nature* **507**, 492–495 (2014).
30. S. Bennett et al., *Mar. Freshw. Res.* **67**, 47–56 (2016).

ACKNOWLEDGMENTS

This work was funded by the Australian Research Council (T.W., G.A.K.), the Hermon Slade Foundation (T.W., S.B.), a U.K. Natural Environment Research Council Independent Research Fellowship (D.A.S.), the Australian Institute of Marine Science (T.W., M.D., B.R.), the Australian National University (C.J.F.), the Western Australian Museum (J.F.), the Department of Parks and Wildlife (T.H.H., S.W.), CSIRO Oceans and Atmosphere (R.C.B., F.D.,

M.A.V.), Fisheries Research and Development Corporation project no. 2008/013 (R.K.H., G.A.K.), The Marsden Fund of The Royal Society of New Zealand (M.S.T.), and the WA Strategic Research Fund for the Marine Environment (R.B., M.A.V., J.F.). T.W. and S.B. conceptualized and wrote the manuscript; T.W., S.B., R.B., T.d.B., K.C., M.D., F.D., J.F., C.J.F., J.S.-G., R.K.H., E.S.H., T.H.H., G.K., B.R., B.J.S., D.K.S., M.T., C.T., F.T., M.A.V., and S.W. provided data; and T.W., S.B., R.K.H., J.S.-G., and D.A.S. performed analyses and modeling. All authors discussed the results and commented on the manuscript. The data are provided in the supplementary materials. Additional information can be obtained from T.W. All authors declare no conflicting interests.

SUPPLEMENTARY MATERIALS

www.sciencemag.org/content/353/6295/169/suppl/DC1
Materials and Methods
Figs. S1 to S3
Tables S1 to S6
References (31–70)

18 January 2016; accepted 31 May 2016
10.1126/science.aad8745

STRUCTURAL BIOLOGY

Structural basis for membrane anchoring of HIV-1 envelope spike

Jyoti Dev,^{1,2*} Donghyun Park,^{3*} Qingshan Fu,¹ Jia Chen,^{3,4} Heather Jiwon Ha,^{3,4} Fadi Ghantous,⁵ Tobias Herrmann,² Weiting Chang,³ Zhijun Liu,⁶ Gary Frey,^{3,4} Michael S. Seaman,⁵ Bing Chen,^{3,4†} James J. Chou^{1,6}

HIV-1 envelope spike (Env) is a type I membrane protein that mediates viral entry.

We used nuclear magnetic resonance to determine an atomic structure of the transmembrane (TM) domain of HIV-1 Env reconstituted in bicelles that mimic a lipid bilayer. The TM forms a well-ordered trimer that protects a conserved membrane-embedded arginine. An amino-terminal coiled-coil and a carboxyl-terminal hydrophilic core stabilize the trimer. Individual mutations of conserved residues did not disrupt the TM trimer and minimally affected membrane fusion and infectivity. Major changes in the hydrophilic core, however, altered the antibody sensitivity of Env. These results show how a TM domain anchors, stabilizes, and modulates a viral envelope spike and suggest that its influence on Env conformation is an important consideration for HIV-1 immunogen design.

HIV-1 envelope spike [Env; trimeric (gp120)₃, cleaved to (gp120/gp41)₃] fuses viral and host cell membranes to initiate infection (1). Binding of gp120 to receptor (CD4) and co-receptor (e.g., CXCR4) trigger large conformational changes, leading to a cascade of refolding events in gp41 and ultimately to membrane fusion (2–4).

Mature Env spikes, (gp120/gp41)₃, are the sole antigens on the virion surface; they often induce strong antibody responses in infected individuals (5, 6). A vast amount of structural information is available for the ectodomain of Env, a primary target of the host immune system, but much less for its transmembrane domain (TMD), membrane-proximal external region (MPER), and cytoplasmic tail (CT), in the context of lipid bilayer. The cryo-EM (electron microscopy) structure of a detergent-solubilized clade B JR-FL EnvΔCT construct without the CT has been described recently (7), but its MPER and TMD are disordered, probably because detergent micelles failed to mimic a membrane environment.

The HIV-1 TMD is more conserved than a typical membrane anchor (fig. S1). Previous studies showed that mutations and truncations in the TMD indeed affect membrane fusion and viral infectivity (8–11). Presence of a GxxxG motif, often implicated in oligomeric assembly of TM helices (12), suggests clustering of TMDs in membrane

(fig. S1). The presence of a conserved, positively charged residue (usually arginine) near the middle of the TMD suggests functions other than just spanning a bilayer. TM helices of many cell surface receptors are not merely inert anchors but play essential roles in receptor assembly and signal transmission. For example, we have shown that CT truncation affects the antigenic surface of the ectodomain of HIV-1 Env on the opposite side of the membrane (13). Thus, understanding the physical coupling (conformation and/or dynamics) between the CT and the ectodomain mediated by the TMD may guide design of immunogens that mimic native, functional Env and induce broadly neutralizing antibodies (bnAbs).

To characterize the TMD structure by nuclear magnetic resonance (NMR), we used a fragment of gp41 (residues 677 to 716; HXB2 numbering, fig. S1), derived from a clade D HIV-1 isolate 92UG024.2 (14). This construct, gp41^{HIV(D677-716)}, contains a short stretch of MPER (residues 677 to 683); the TM segment (residues 684 to 705), defined by hydrophobicity; and a fragment previously assigned to the CT domain [residues 706 to 716, containing a tyrosine-based sorting motif (15, 16)]. The gp41^{HIV(D677-716)} protein was purified and reconstituted into bicelles (fig. S2, A and B) (17–19) with an expected lipid-bilayer diameter of ~44 Å (fig. S2C) (20, 21), thereby incorporating the refolded gp41^{HIV(D677-716)} into a membrane-like environment. The bicelle-reconstituted gp41^{HIV(D677-716)} migrated on SDS-polyacrylamide gel electrophoresis (SDS-PAGE) with a size close to that of a trimer (theoretical molecular mass 14.1 kDa) (fig. S2D), suggesting that the protein was trimeric and resistant to SDS denaturation. The reconstituted gp41^{HIV(D677-716)} protein in bicelles generated an NMR spectrum with excellent chemical-shift dispersion (fig. S3A). The equivalent protein constructs from isolates 92BR025.9 (clade C) and 92RU131.16 (clade G) gave similar NMR spectra (fig. S3, B and C), suggesting that the TMDs of most HIV-1 Envs have similar structures when reconstituted in bicelles. We completed the NMR structure of gp41^{HIV(D677-716)} using a previously described protocol (figs. S4 and S5) (22, 23). The

¹Department of Biological Chemistry and Molecular Pharmacology, Harvard Medical School, 250 Longwood Avenue, Boston, MA 02115, USA. ²Virology Program, Harvard Medical School, 260 Longwood Avenue, Boston, MA 02115, USA. ³Division of Molecular Medicine, Boston Children's Hospital, 3 Blackfan Street, Boston, MA 02115, USA. ⁴Department of Pediatrics, Harvard Medical School, 300 Longwood Avenue, Boston, MA 02115, USA. ⁵Center for Virology and Vaccine Research, Beth Israel Deaconess Medical Center, 330 Brookline Avenue, Boston, MA 02115, USA. ⁶State Key Laboratory of Molecular Biology, National Center for Protein Science Shanghai, Shanghai Institute of Biochemistry and Cell Biology, Chinese Academy of Sciences, Shanghai 200031, China.

*These authors contributed equally to this work. †Corresponding author. Email: bchen@crystal.harvard.edu

Climate-driven regime shift of a temperate marine ecosystem

Thomas WernbergScott BennettRussell C. BabcockThibaut de BettigniesKatherine CureMartial DepczynskiFrancois DufoisJane FromontChristopher J. FultonRenae K. HoveyEuan S. HarveyThomas H. HolmesGary A. KendrickBen RadfordJulia Santana-GarconBenjamin J. SaundersDan A. SmaleMads S. ThomsenChenae A. TuckettFernando TuyMathew A. VanderkliftShaun Wilson

Science, 353 (6295), • DOI: 10.1126/science.aad8745

No turning back?

Ecosystems over time have endured much disturbance, yet they tend to remain intact, a characteristic we call resilience. Though many systems have been lost and destroyed, for systems that remain physically intact, there is debate as to whether changing temperatures will result in shifts or collapses. Wernburg *et al.* show that extreme warming of a temperate kelp forest off Australia resulted not only in its collapse, but also in a shift in community composition that brought about an increase in herbivorous tropical fishes that prevent the reestablishment of kelp. Thus, many systems may not be resilient to the rapid climate change that we face.

Science, this issue p. 169

View the article online

<https://www.science.org/doi/10.1126/science.aad8745>

Permissions

<https://www.science.org/help/reprints-and-permissions>

Use of this article is subject to the [Terms of service](#)